

Recording Device for Natural Haptic Textures Felt with the Bare Fingertip

Jonathan Platkiewicz^{1,3}, Alessandro Mansutti²,
Monica Bordegoni², and Vincent Hayward³

¹ Sibley School of Mechanical and Aerospace Engineering,
Cornell University, Ithaca, NY 14853, USA,
jonathan.platkiewicz@gmail.com

² Dipartimento di Meccanica, Politecnico di Milano,
Via La Masa, 20156 Milan, Italy,

mansutti.alessandro@gmail.com, monica.bordegoni@polimi.it

³ Sorbonne Universités, UPMC Univ Paris 06, UMR 7222, ISIR,
F-75005, Paris, France.
hayward@isir.upmc.fr

Abstract. The perception of haptic textures depends on the mechanical interaction between a surface and a biological sensor. A texture is apprehended by sliding one's fingers over the surface of an object. We describe here an apparatus that makes it possible to record the mechanical fluctuations arising from the friction between a human fingertip and easily interchangeable samples. Using this apparatus, human participants tactually scanned material samples. The analysis of the results indicates that the biomechanical characteristics of individual fingertips clearly affected the mechanical fluctuations. Nevertheless, the signals generated for a single material sample under different conditions showed some invariant features. We propose that this apparatus can be a valuable tool for the analysis of natural haptic surfaces.

Keywords: texture, biotribology, biomechanics, apparatus, humans.

1 Introduction

In vision and in audition, the importance of considering the structure of natural scenes to better understand the organization of the nervous system has been extensively developed and studied, and have led to groundbreaking results in neurophysiology [8, 13]. Very few studies of natural haptic scenes, and of textures in particular, have been undertaken, however. Studies about natural haptic textures are either strictly psychophysical [3, 10, 22], neurophysiological [18], or robotic [2, 7, 9]. To our knowledge, there has been no study regarding the physical determinants of the interaction between a human fingertip and a complex surface, known to depend on so many rich physico-chemical phenomena [1], save for correlates of the sensation of pleasantness [11].

This gap can be explained by the limitations of the available techniques for recording natural haptic textures. A visual scene can be recorded by a camera,

an auditory scene can be recorded by a microphone, but there is no standardized device or method to record a haptic texture elicited through finger exploration. Several apparatuses have been recently developed for similar ends [4, 6, 19], but they are based on an artificial probe as a haptic sampler. . Nevertheless, interesting approaches involved the measurement of the acoustic emissions due to a finger sliding on a surface or measurements through vibrometers [12, 15]. In this study, we adapted an apparatus developed in [20] that has the advantage of leaving the finger free of any mechanical interference, owing to finger movement restrictions or devices attached to the anatomy.

It has been shown that haptic texture perception is a multi-dimensional process that does not only depend on the microgeometry of tactually explored surface, but also on the tribology of finger pad-surface interaction on the mechanics of fingertip pulp [1, 20]. Therefore, haptic texture recordings that use a robotic finger or a probe are liable to miss critical aspects of this process. In this study, we described an apparatus specifically designed for capturing and quantifying the detailed physics underlying texture perception when a human finger is spontaneously exploring a surface. We studied several typical cases, by varying the haptic sampler or the explored material. We performed several recordings where a human participant was asked to spontaneously slide her finger or a rigid probe on various surfaces, but not asked to report her sensation. We emphasized here on the importance of the sampler and the sampler-surface contact on the produced vibration that can be encoded by the mechanoreceptors, and not on the perceptual process. Our objective was to demonstrate that a natural haptic texture should consist of a naturally produced friction between a fingertip and a surface, and not of a surface microgeometry only.

2 Materials and Methods

The experimental setup. As shown in Figure 1, the main components of the setup comprise a mechanical system for material sample plates fixation, a position measurement device, and a specifically designed friction force transducer. The mechanical system takes advantage of a lever system to easily insert, fixate, and remove a 10 cm x 10 cm plate. The plate was fixed during a slide, and could be changed between slides. The position measurement device consists of a string potentiometer of very high accuracy, $\approx 10 \mu\text{m}$ (WPS-250-MK30-P10, Micro-Epsilon, Ortenburg, Germany). The restriction of the participant's finger movement in a single direction allowed us to use a single string potentiometer (cf. Task). To compensate the retraction force exerted by the string potentiometer, we introduced a counter-weight of 250 g at the other end of the string. The force transducer and the charge amplifiers are the ones used in [20].

Task. We used as stimulus texture a matt glass and a structured floor tile, taken from the set of materials collected and studied in [3]. These two samples were chosen for their typical perceptual properties: the matt glass is one of the smoothest textures of the set (averaged roughness: $5.2 \mu\text{m}/\sqrt{\text{mm}^{-1}}$; compressibility, $67/\text{m}/\text{m}^2$, as measured in [3]), and the structured floor tile is one of the

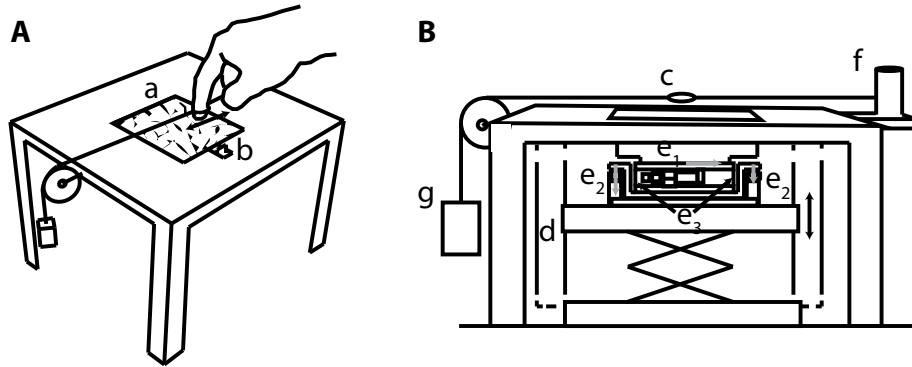


Fig. 1. Experimental setup. A: Participants run their finger over a sample (a) clamped to the measurement bench (b). The finger is inserted in a ring maintained by strings (c). The plate is removable and its height adjustable (d). B: The device measures frictional force (arrows in gray) by three piezoelectric force transducers (e): one transducer measured the tangential component of the force (e_1), the two others measured its normal component (e_2). The two leaf springs (e_3) allow motion in the horizontal direction only. The finger position along the sliding direction is measured with high accuracy by a string potentiometer (f). The traction force exerted by the string of the potentiometer is counter-balanced (g).

roughest textures of the set (averaged roughness: $15 \mu\text{m}/\sqrt{\text{mm}^{-1}}$; compressibility, $25 \text{ 67}/\text{m}/\text{m}^2$, as measured in [3]).

Three conditions were tested with a single participant (1 female, of age 25), each lasting 5 s: the participant was asked to slide the bare index finger of her dominant hand over the material sample using a back-and-forth motion at steady speed (see Figure 1A); the same task but the finger was covered with talc; the same task but the participant used a pen instead of her finger to scan the surface.

Data analysis. In this study, we considered the tangential friction force, F_T , the normal friction force, F_N , and their ratio, $\mu(t) = F_T(t)/F_N(t)$. This last dimensionless parameter can be considered as an instantaneous kinetic friction coefficient. For all the analysis described below, we only considered the fluctuation of the instantaneous kinetic friction coefficient, $\delta\mu = \mu - \langle\mu\rangle$, where “ $\langle\cdot\rangle$ ” denotes the average with respect to x . Following the methods used by [21], the temporal signal, $\delta\mu(t)$, was resampled in the spatial domain. This reparameterization can be justified by noting that the inverse problem of texture perception consists of recovering the microtopography of a material’s surface from the friction between a haptic sampler and the surface. The Fourier analysis of the resampled spatial signal, $\delta\mu(x)$, followed the methods used in [21]. A fast Fourier transform was performed on a signal, after having applied a 8th-order Butterworth high-pass filter with a cutoff frequency of 0.01 mm^{-1} to the signal (note that the cutoff frequency corresponds to a wavelength of 100 mm, the width of a material sample plate). The high-pass filtering helps to ensure that the oscillatory motion

of the arm during the sliding is not taken into account by the Fourier analysis. The cross-correlation analysis was performed on the same signals than the ones processed in the Fourier analysis ($\delta\mu(x)$). We computed the normalized cross-correlation for two signals obtained in two distinct experimental conditions of the three tested ones (bare finger, talc-covered finger, and probe).

3 Results and Discussion

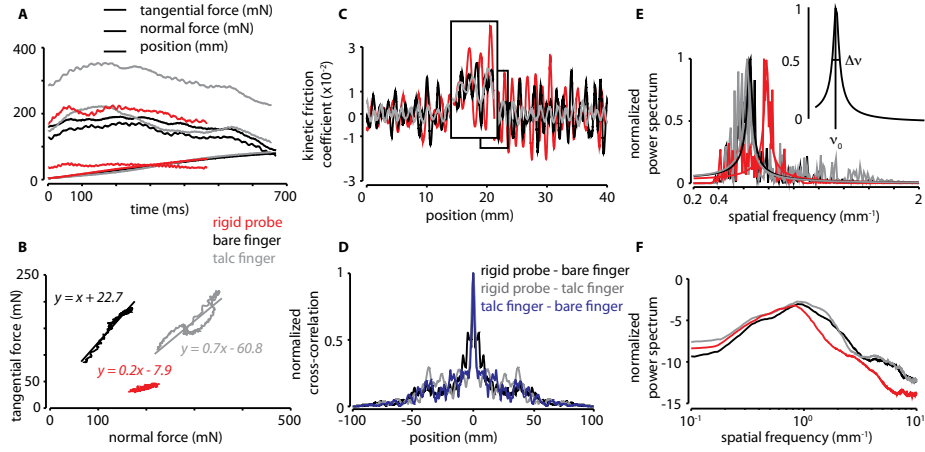


Fig. 2. Effect of the recording conditions. Black, grey, and red colors respectively indicate data obtained in the bare finger, in the talc-covered finger, and in the rigid probe conditions. A: Temporal variation of the tangential force (solid line), the normal force (dashed line), and the fingertip position (dotted line). B: Correlation between the instantaneous tangential sliding force and the instantaneous normal sliding force for each scanning condition. A solid line represents the linear regression of a given correlation. C: Spatial variation of the fluctuating part of the kinetic friction coefficient, $\delta\mu(x) = \mu(x) - \langle\mu\rangle$. D: Envelope of the absolute value of the normalized cross-correlation between signals, $\delta\mu(x)$, obtained in two of the three scanning conditions. E: Normalized power spectrum of $\delta\mu(x)$. The thick line represents the regression of the power spectrum by the function, $y(x) = 2\zeta\nu_n^2/\sqrt{(x^2 - \nu_n^2)^2 + (2\zeta\nu_n x)^2}$. The illustration on the upper right corner shows the geometric representation of the fitting parameters ($\zeta = \Delta\nu/(2\nu_0)$ and $\nu_n = \nu_0/\sqrt{1 - \zeta^2}$). F: Moving average of the logarithm of the normalized power spectrum of $\delta\mu(x)$ with the spatial frequency in logarithmic scale.

Tribological analysis. We estimated the kinetic friction coefficient from the measured tangential and normal components of the friction force, as shown in Figures 2B and 3B. For that, we performed a linear regression on the relationship between the instantaneous tangential friction force, $F_T(t)$, and the instantaneous normal friction force, $F_N(t)$, obtained in the different experimental conditions for

the two selected material samples. We measured for the dimensionless slope with the matt glass surface: under the bare finger condition, 1.02 (with a coefficient of the determination for the linear regression, $r^2 = 0.95$); under the talc condition, 0.75 ($r^2 = 0.77$); and under the probe condition, 0.23 ($r^2 = 0.79$). For the structured floor tile surface, we obtained: under the bare finger condition, 0.43 ($r^2 = 0.51$); under the talc condition, 0.58 ($r^2 = 0.86$); and under the probe condition, 0.18 ($r^2 = 0.18$). For all these regression analyses, we measured a p -value of zero, which confirms the statistical significance of the linear regression. For the two tested materials, the measured slope is much smaller in the probe condition than in the bare finger condition. This result confirms that the tribological properties of the contact, as estimated by the measured slope, can be affected by the system used for scanning a material's surface. It confirms the hypothesis that it is critical to involve human bare finger in the study of natural texture perception. Interestingly, whereas the friction coefficient changed significantly between the two material samples for the bare finger condition, it barely changed for the talc condition. This confirms that talc makes a finger contact closer to Coulombic dry friction, and that the bare finger-surface contact is poorly described by a dry friction model [1].

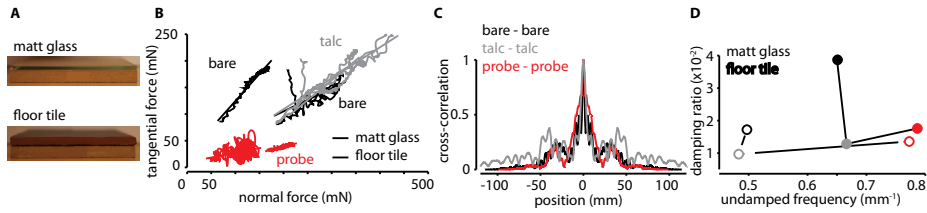


Fig. 3. Effect of the material properties. Same color code as in Figure 2 for the scanning conditions. Solid and dashed lines correspond respectively to results for the matt glass and the floor tile surfaces. A: Material samples. B: Correlation between the instantaneous tangential sliding force and the instantaneous normal force for each material and each scanning condition. A line represents the linear regression for a given correlation. C: Envelope of the absolute value of the normalized cross-correlation between signals, $\delta\mu(x)$, obtained with the two different material samples for each haptic sampler. D: Results of the fit of the normalized power spectrum (cf. Spectral Analysis). The filled and empty dots correspond respectively to the matt glass and the structured floor tile surfaces, and the lines relate the data points for a given material's surface.

Spectral analysis. We observed that the power spectra of all recorded vibration signals, $\delta\mu(x) = \mu(x) - \langle \mu(x) \rangle$, can be accurately described around its peak by the function, $y = 2\zeta\nu_n^2 / \sqrt{(\nu^2 - \nu_n^2)^2 + (2\zeta\nu_n\nu)^2}$, typical of a damped harmonic oscillator of undamped frequency, ν_n , and damping ratio, ζ ($\zeta = \Delta\nu / (2\nu_0)$, with $\Delta\nu$ the half-power bandwidth and ν_0 the resonance frequency; additionally, $\nu_0 = \nu_n \sqrt{1 - \zeta^2}$). The nonlinear regression gave for the matt glass surface:

$\nu_n = 0.65 \text{ mm}^{-1}$ and $\zeta = 2.6 \cdot 10^{-2}$ for the bare finger ($r^2 = 0.76$); $\nu_n = 0.63 \text{ mm}^{-1}$ and $\zeta = 2.8 \cdot 10^{-2}$ for the talc-covered finger ($r^2 = 0.49$); $\nu_n = 0.78 \text{ mm}^{-1}$ and $\zeta = 1.8 \cdot 10^{-2}$ for the rigid probe ($r^2 = 0.73$). Similarly, we obtained for the structured floor tile surface: $\nu_n = 0.39 \text{ mm}^{-1}$ and $\zeta = 3 \cdot 10^{-2}$ for the bare finger ($r^2 = 0.51$); $\nu_n = 0.45 \text{ mm}^{-1}$ and $\zeta = 1.4 \cdot 10^{-2}$ for the talc-covered finger ($r^2 = 0.54$); $\nu_n = 0.76 \text{ mm}^{-1}$ and $\zeta = 1.3 \cdot 10^{-2}$ for the rigid probe ($r^2 = 0.8$). For all these regression analyses, we measured a p -value of zero, which confirms the statistical significance of the chosen regression. Interestingly, the representation provided by this regression (see Figure 3D) shows that the relative characteristic between the scanning conditions is preserved despite the change of surface. In addition, we observed a strong similarity between the vibration signals obtained under the different scanning conditions but a single surface, as shown in the cross-correlation analysis of Figure 2D, which supports the hypothesis that texture perception can be robust with respect to the scanning mode [22]. We can note in Figure 3C that there is a stronger similarity between signals under the rigid probe condition than under the talc-covered finger condition, which confirms that texture discrimination is more than discriminating surface's microtopography.

An interpretation of this regression result in the Fourier analysis could be that it reflects the viscoelasticity of the fingertip's skin [14, 16]. Under this hypothesis, the undamped frequency, ν_n , would scale with the skin's equivalent elastic modulus, and the damping ratio, χ , with the skin's equivalent viscosity. Highly similar values were observed for the fitting parameters under the bare finger and the talc-covered finger conditions, confirming the viscoelasticity hypothesis as talc modifies the finger-surface tribology only, and not the skin mechanics. Nevertheless, it was also possible to describe the power spectrum obtained under the rigid probe condition with such function, but with a clearly distinct undamped frequency. Another interpretation of this result would be that it reflects the fingerprint pattern of the fingertip's skin. This pattern has been indeed proposed to induce a Gabor filter on the surface microgeometry [17], which also exhibits a band-pass filter property. Using an elastomer whose surface is patterned with parallel ridges mimicking the fingerprints, it was shown that the frequency at the peak of the power spectrum, ν_0 , is given by the inverse of the interridge distance, $\nu_0 = 2\pi/\lambda$. Under this hypothesis, our results in the bare finger condition would predict an interridge distance of, $\lambda \approx 1.5 \text{ mm}$, fairly close to the typical value ($\approx 0.5 \text{ mm}$). However, we measured similar values for the frequency at peak under the talc-covered finger and bare finger conditions, even though the talc fills the interridge gap, which should impact the inferred interridge value. As suggested by [5], it is possible that the patterned elastomer model does not fully capture the complexity of the skin structure.

Wiertlewski et al. observed that the power spectrum of the vibration signal generated by the slip of a human finger over a smooth, flat, but not mirror-finish surface followed a $1/f$ trend [21]. The apparatus employed here was based on a similar principle than the one they used, and we applied a similar methodology for analyzing the friction signals. We filtered these signals using a high-pass filter of cutoff spatial frequency, 0.01 mm^{-1} (i.e. 100 mm spatial periods), re-

moving thus the low-frequency components of the signal's energy. This filtering was motivated by the observation that dissimilarity between textures were not well reflected in our measurements. We hypothesized that the texture signal was dominated in the low frequency range by the signal induced by the oscillatory movement of the arm. Interestingly, the observation that the textures can be well discriminated after high-pass filtering suggests that there are two main contributions to the signal characteristic of a haptic texture, the hand's exploratory movement and the friction induced oscillations. This confirms the importance of involving active motion in the study of touch, since passive touch would inform the brain of only the high-frequency components arising from mechanical interactions.

4 Conclusion

We described an apparatus that can be used for quantifying the different contributing factors to texture perception: the sampler-surface tribology, the sampler mechanics, and the material's surface microtopography. Unlike traditional haptic texture recording devices, our recording involves the friction between a human fingertip and any material's surface, and an oscillatory motor behavior typically observed during surface haptic exploration. In this study, we emphasized that a natural haptic texture consists of the friction between a fingertip and natural material's surface. The developed apparatus can thus be used for investigating the structure and the statistics of natural haptic textures, supposed to be a critical constraint on the somatosensory system.

Acknowledgments. The authors are grateful to W. M. Bergmann Tiest for lending us the set of material samples and R. Pijewski, S.-C. Wong, and R. Singal Reddy for the design and construction of the experimental setup. We thank V. Balasubramaniam, A. Hermundstad, K. Krishnamurthy, and Y. Visell for fruitful discussions; and M. Wiertelwski for assistance with the numerical analysis. We acknowledge the support of the European Research Council, Advanced Grant PATCH, (No. 247300), and of the Fulbright Scholar Program.

References

1. M. J. Adams, S. Johnson, P. Lefèvre, V. Lévesque, V. Hayward, T. André, and J. Thonnard. Finger pad friction and its role in grip and touch. *J. R. Soc. Interface*, 10(80), 2013.
2. W. Adi and S. Sulaiman. Texture classification using wavelet extraction: An approach to haptic texture searching. In *C.I.T.I.S.I.A.*, pages 434–439. IEEE, 2009.
3. W. M. Bergmann Tiest and A. M. L. Kappers. Analysis of haptic perception of materials by multidimensional scaling and physical measurements of roughness and compressibility. *Acta psychol.*, 121(1):1–20, 2006.
4. M. R. Cutkosky, R. D. Howe, and W. R. Provancher. Force and tactile sensors. *Springer Handbook of Robotics*, pages 455–476, 2008.

5. R. S. Dahiya and M. Gori. Probing with and into fingerprints. *J. Neurophysiol.*, 104(1):1–3, 2010.
6. R. S. Dahiya, G. Metta, M. Valle, and G. Sandini. Tactile sensing—from humans to humanoids. *IEEE T. Robot.*, 26(1):1–20, 2010.
7. J. A. Fishel and G. E. Loeb. Bayesian exploration for intelligent identification of textures. *Front. Neurobot.*, 6, 2012.
8. W. S. Geisler. Visual perception and the statistical properties of natural scenes. *Annu. Rev. Psychol.*, 59:167–192, 2008.
9. P. Giguere and G. Dudek. A simple tactile probe for surface identification by mobile robots. *IEEE T. Robot.*, 27(3):534–544, 2011.
10. M. Hollins, S. Bensmaïa, K. Karlof, and F. Young. Individual differences in perceptual space for tactile textures: Evidence from multidimensional scaling. *Percept. Psychophys.*, 62(8):1534–1544, 2000.
11. A. Klöcker, M. Wiertelwski, V. Théate, V. Hayward, and J.-L. Thonnard. Physical factors influencing pleasant touch during tactile exploration. *PLoS ONE*, 8(11):e79085, 2013.
12. F. Martinot, A. Houzefa, and C. Biet, M. and Chaillou. Mechanical responses of the fingerpad and distal phalanx to friction of a grooved surface: Effect of the contact angle. In *H.A.P.T.I.C.S.*, pages 297–300. IEEE, 2006.
13. J. H. McDermott and E. P. Simoncelli. Sound texture perception via statistics of the auditory periphery: evidence from sound synthesis. *Neuron*, 71(5):926–940, 2011.
14. G. Moy, U. Singh, E. Tan, and R. S. Fearing. Human psychophysics for teletaction system design. *Haptics-e*, 1(3):1–20, 2000.
15. Y. Tanaka, Y. Horita, A. Sano, and H. Fujimoto. Tactile sensing utilizing human tactile perception. In *Proc. W.H.C.*, pages 621–626. IEEE, 2011.
16. C. L. Van Doren. A model of spatiotemporal tactile sensitivity linking psychophysics to tissue mechanics. *J. Acoust. Soc. Am.*, 85(5):2065–2080, 1989.
17. E. Wandersman, R. Candelier, G. Debrégeas, and A. Prevost. Texture-induced modulations of friction force: the fingerprint effect. *P.R.L.*, 107(16):164301, 2011.
18. A. I. Weber, H. P. Saal, J. D. Lieber, J.-W. Cheng, L. R. Manfredi, J. F. Dammann, and S. J. Bensmaïa. Spatial and temporal codes mediate the tactile perception of natural textures. *P.N.A.S.*, 110(42):17107–17112, 2013.
19. M. Wiertelwski. *Reproduction of Tactile Textures: Transducers, Mechanics and Signal Encoding*. Springer, 2013.
20. M. Wiertelwski, S. Endo, A. M. Wing, and V. Hayward. Slip-induced vibration influences the grip reflex: A pilot study. In *Proc. W.H.C.*, pages 627–632, 2013.
21. M. Wiertelwski, C. Hudin, and V. Hayward. On the 1/f noise and non-integer harmonic decay of the interaction of a finger sliding on flat and sinusoidal surfaces. In *Proc. W.H.C.*, pages 25–30. IEEE, 2011.
22. T. Yoshioka, S. J. Bensmaïa, J. C. Craig, and S. S. Hsiao. Texture perception through direct and indirect touch: an analysis of perceptual space for tactile textures in two modes of exploration. *Somatosens. Mot. Res.*, 24(1-2):53–70, 2007.